Solid-state chemistry of early transition-metal oxides containing d^0 and d^1 cations†

Nattamai S. P. Bhuvanesh and Jagannatha Gopalakrishnan

Solid State and Structural Chemistry Unit, Indian Institute of Science, Bangalore 560 012, India

This paper presents a brief survey of the structures and properties of early transition-metal oxides containing d^0 and d^1–d^0 electronic configurations. The metal–oxygen (MO_6) octahedron, which is the essential structure building unit of these materials, exhibits a characteristic out-of-centre distortion for the d^0 configuration in many instances, the degree of distortion increasing with decreasing HOMO–LUMO gap. Several characteristic properties of d^0 oxides, which include low-dimensional structures (that give rise to intercalation, ion-exchange and acidity), ferroelectricity and non-linear optical response, arise from the out-of-centre distortion of d^0 MO_6 octahedra. Oxides containing d^1–d^0 electronic configurations exhibit an equally impressive array of electronic properties that owe their origin to the nature of d states near the Fermi level. While three-dimensional (3-D) oxides containing 5d and 4d electrons exhibit itinerant electron properties, $3d^1$ oxides, especially with low-dimensional (low-D) structures, display localized electron magnetism and semiconduction. Low-dimensional oxides containing 4d electrons, typified by molybdenum bronzes and Mo_4O_{11}, exhibit charge-density-wave (CDW)-driven electronic instabilities arising from electron–phonon interactions.

Transition-metal oxides constitute a fascinating class of inorganic solids[1] that have attracted the attention of solid-state/materials chemists from the early days.[2,3] Among them, oxides of the early transition-metals (periodic groups 4, 5, 6 and 7) containing d^0 and d^1 electronic configuration are a special subclass, distinctly different from the other transition-metal oxides, showing several unique features. For example, the crystal structures of d^0 metal oxides[4] consist of distorted metal–oxygen (MO_6) octahedra where the cation is displaced from the centre of the octahedron (Fig. 1). Several of the interesting features of these oxides can be directly traced to this distortion. The occurrence of layered structures[5] and distinct oxide hydrates[5] for V_2O_5, MoO_3 and Re_2O_7 is a direct consequence of the distortion. The high static relative permittivity and the consequent ferroelectric behaviour, the presence of soft phonon modes[6] and the ability to accommodate oxygen-deficient non-stoichiometry (*e.g.* WO_{3-x}, TiO_{2-x}) without oxygen vacancies could all be traced to a soft M—O potential[7] that is again a direct consequence of the out-of-centre distortion of MO_6 octahedra in d^0 metal oxides. Another special feature is that the d^0 cation, which is in its highest oxidation state, can be reduced partially or wholly in many instances, where the electronic configuration of the metal is now d^1/d^0 or d^1. Two classes of reduced oxides containing d^1/d^0 configuration are well known. They are the oxide bronzes[8] typified by the tungsten bronzes, A_xWO_3 (A = alkali metal), which exhibit metal-like properties and the reduced oxides[9] such as WO_{3-x} and TiO_{2-x} with an apparent anion deficiency. A unique structural principle called crystallographic shear (CS) that operates in the latter materials eliminates the oxygen vacancies without changing the octahedral coordination of the metal atom; as a consequence, highly ordered homologous series of mixed-valent phases of the formulae, W_nO_{3n-1}, W_nO_{3n-2} and Ti_nO_{2n-1}, are obtained instead of grossly non-stoichiometric phases.[9,10] Well known among the oxides containing d^1 electronic configuration are Ti_2O_3, VO_2 and ReO_3. Besides these early transition-metal oxides which have been known for quite some time, several new binary and multinary ones have been uncovered in the recent decades. In addition to the ferroelectric (d^0) and metallic (d^1–d^0) properties to which we have already referred, these oxides exhibit a whole range of interesting materials properties that include Brønsted acidity,[11] catalytic[12] and photocatalytic[13] reactivity, non-linear optical response,[14] metal–non-metal transitions,[15,16] charge-density-wave instability[17] and superconductivity.[18]

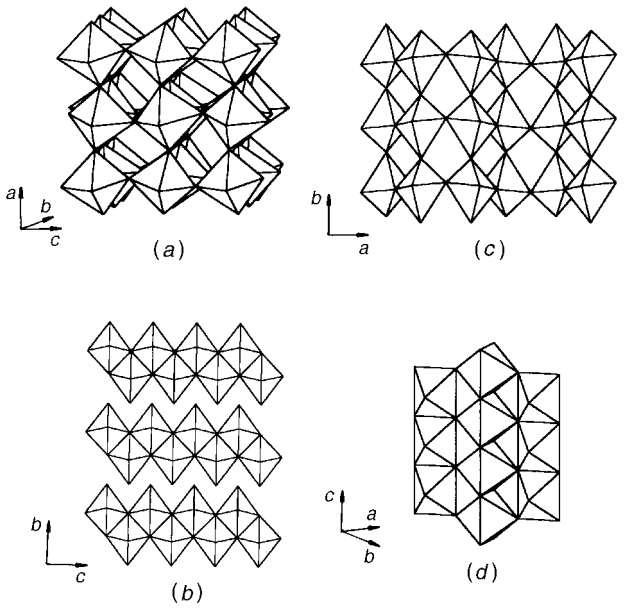

Fig. 1 Representative structures of d^0 oxides: (*a*) monoclinic WO_3, (*b*) MoO_3, (*c*) V_2O_5 and (*d*) TiO_2 (rutile)

The purpose of this paper is to focus attention on the structure and properties of early transition metal oxides containing d^0 and d^1–d^0 cations, especially on the recent developments, and to point out potential new directions in this growing area of inorganic materials chemistry.

† Contribution No. 1273 from the Solid State and Structural Chemistry Unit.

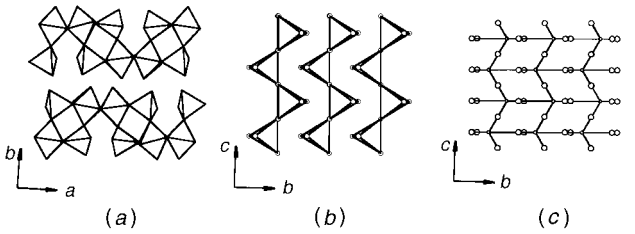

Fig. 2 Structures of (*a*) Re_2O_7 and (*b*) CrO_3. In (*c*), the atomic positions of the CrO_3 structure are shown, revealing the highly distorted octahedral coordination around Cr^{VI}.

d^0 Oxides

Early transition metals of the periodic groups 3‡–7, whose valence electrons are well screened by the rare-gas inner core and hence readily ionized, form d^0 oxides where the metal atom is in its highest oxidation state. The following are the well known binary oxides containing d^0 cations:[5] TiO_2, ZrO_2, HfO_2; V_2O_5, Nb_2O_5, Ta_2O_5; CrO_3, MoO_3, WO_3; Mn_2O_7, Tc_2O_7, Re_2O_7. The structures of many of these oxides (TiO_2, V_2O_5, Nb_2O_5, MoO_3 and WO_3) are built up of MO_6 octahedra which are connected through corners and edges.[4] The structures of other oxides consist of different polyhedra: while ZrO_2 and HfO_2 contain MO_7 polyhedra, Ta_2O_5 consists of both TaO_6 octahedra and TaO_7 pentagonal bipyramids. The structures of CrO_3, Mn_2O_7 and Tc_2O_7 consist of only MO_4 tetrahedra. The unique layered structure of Re_2O_7 on the other hand contains corner-sharing ReO_6 octahedra and ReO_4 tetrahedra.[5] We show in Fig. 1 and 2 representative structures§ of d^0 oxides.

A characteristic feature of all the octahedral structures is that the d^0 MO_6 octahedra are considerably distorted in such a way that the cation is displaced from the centre of the octahedron creating unequal M—O bonds.[19] With the V_2O_5 structure, one of the V—O bonds is so long (2.79 Å) that the oxygen coordination around vanadium can be regarded as square pyramidal rather than octahedral.[20] Similarly, although the structure of CrO_3 is conventionally described as consisting of chains of $CrO_2O_{2/2}$ tetrahedra,[21] inclusion of two additional oxygens from adjacent chains would give a highly distorted octahedral coordination around Cr^{VI} (Fig. 2). We see that the characteristic out-of-centre distortion of MO_6 octahedra in d^0 oxides increases with increasing charge-to-size ratio of the cations.

Out-of-centre distortions of MO_6 octahedra in d^0 oxides, which are crucial to many of the interesting properties of these materials, have an electronic origin.[22] To understand the origin, let us consider the electronic structure of a typical d^0 oxide, *viz*., WO_3, in its undistorted form (Fig. 3). The valence band (which corresponds to the highest occupied molecular orbitals, HOMOs) is mainly anionic (oxygen 2s and 2p), and the conduction band (which corresponds to the lowest unoccupied molecular orbitals, LUMOs) is mainly cationic, arising from the empty d states. For small and highly charged d^0 cations, the separation between the HOMO and the LUMO states becomes sufficiently small so as to permit a mixing between them that stabilizes the occupied states at the expense of the unoccupied states through a second-order Jahn–Teller effect.[23] The effect manifests in the form of out-of-centre distortion of MO_6 octahedra that gives rise to unsymmetrical M–O···M linkages in extended structures. The smaller the HOMO–LUMO gap, the larger is the distortion. For d^n ($n>0$) configuration, the distortion is rapidly suppressed with increasing n value. The model readily explains the observed structural features of d^0 oxides.[19] Thus, for small and highly charged cations such as V^V, Cr^{VI} and Mo^{VI}, the distortion is large, and for large and relatively less charged cations such as Zr^{IV}, Hf^{IV} and Sc^{III}, there is less or no distortion at all around their MO_6 octahedra. Between cations of same charge and similar size such as Nb^V and Ta^V or Mo^{VI} and W^{VI}, the distortion is lesser for the heavier ions because of the larger HOMO–LUMO gap. In chemical terms, the variation of the HOMO–LUMO gap and hence the distortion of MO_6 octahedra could be related to polarization of anions by highly charged cations. This effect could thus be understood in terms of Pearson's concept[24] of 'hardness'. In ternary and multinary phases containing d^0 cations, the magnitude of the distortion is modulated by the presence of other cations and the actual crystal structure which may either buttress or suppress the effects of distortion.[19]

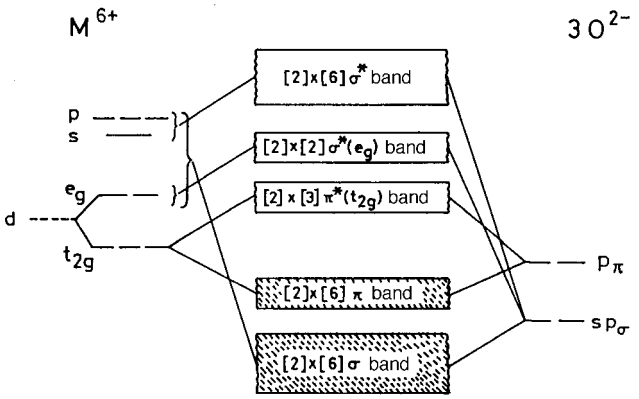

Fig. 3 Schematic electronic structure of an undistorted d^0 MO_3 oxide. This diagram is applicable to hypothetical cubic WO_3. For ReO_3, the additional $5d^1$ electron would occupy the π^* (t_{2g}) band.

We shall now turn to the consequences of the distortion of MO_6 octahedra in d^0 oxides. An obvious consequence is that the oxygens of the long M—O bonds are relatively more ionic (more basic) than the oxygens of the short M—O bonds. The long M—O bonds become vulnerable to scission and the basic oxygens susceptible to electrophilic attack, for example, by protons. Formation of well defined hydrates of WO_3, MoO_3 and Re_2O_7 is a direct manifestation of the reactivity of long M—O bonds of the distorted MO_6 octahedra. Interestingly, the hydrates possess lower dimensionality structures as compared to the parent anhydrous oxides; thus $WO_3{\cdot}H_2O$ is layered,[25] while WO_3 is three-dimensional (Fig. 4). $Re_2O_7{\cdot}2H_2O$ has a molecular structure (Fig. 4), while Re_2O_7 has a layered structure.[26] A more dramatic illustration of the reactivity of long M—O bonds is provided by the formation of layered $MOPO_4$ hydrates (M = V, Nb). Here the anhydrous $MOPO_4$ phases possess a three-dimensional structure[27] consisting of chains of corner-connected MO_6 octahedra with alternating long and short M—O bonds along the chain, while the hydrates possess a layered structure[28,29] where the oxygens of the long M—O bonds are replaced by water of hydration (Fig. 5). Interestingly, the layered oxide hydrates $WO_3{\cdot}H_2O$, $MoO_3{\cdot}H_2O$ and $NbOPO_4{\cdot}H_2O$ and $Nb_{1-x}V_xOPO_4{\cdot}xH_2O$ are all strong Brønsted acids[29–31] intercalating basic organic molecules such as *n*-alkylamines through acid–base interaction:

$$O{=}M{-}OH_2 \rightleftharpoons [O{=}M{-}OH^-]H^+$$

$$[O{=}M{-}OH^-]H^+ + RNH_2 \rightleftharpoons [O{=}M{-}OH^-] + H_3N^+R$$

Another manifestation of the acidity of these oxide hydrates is the formation of higher hydrates,[28,32] $WO_3{\cdot}2H_2O$, $MoO_3{\cdot}2H_2O$, $VOPO_4{\cdot}2H_2O$ and $NbOPO_4{\cdot}xH_2O$ ($x=2$–3),

‡ Although group 3 oxides, Sc_2O_3, Y_2O_3 and La_2O_3, belong to this category, we do not consider them here because of the large separation between the empty d^0 states and filled oxygen 2p and 2s states, which makes the d^0 states chemically inaccessible.

§ The structures are drawn from the crystallographic data given in the literature using ATOMS software.

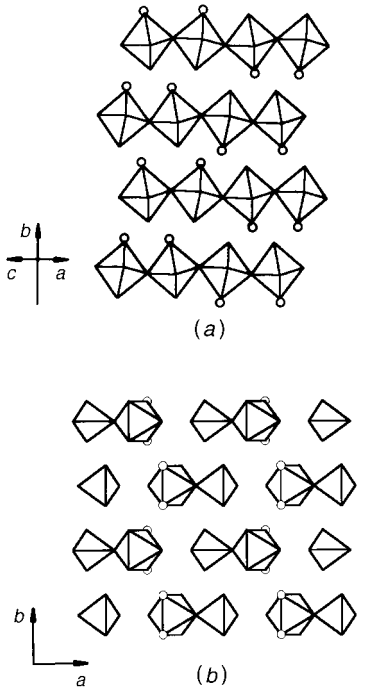

Fig. 4 Structures of (*a*) $WO_3 \cdot H_2O$ and (*b*) $Re_2O_7 \cdot 2H_2O$

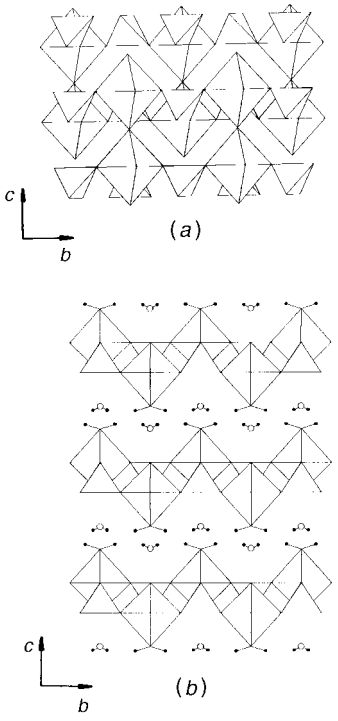

Fig. 5 Structures of (*a*) $VOPO_4$ and (*b*) $VOPO_4 \cdot 2H_2O$

where the additional water molecules are held in between the layers through hydrogen bonding.[33]

The consequences of the short M—O bonds in d^0 oxides are more impressive. Since the oxygen of the shortest M—O bond in a distorted octahedron is acidic relative to other oxygens, protons (or H_3O^+ ions) attached to this oxygen acquire a distinct Brønsted acidity. Several protonated oxides of this kind have been synthesized in recent years. We list them in Table 1 along with their parent alkali-metal analogues from which the protonated derivatives are obtained by ion exchange. Since the parent compounds are all layered, containing alkali-metal cations in the interlayer region, topochemical ion

Table 1 Oxide solid acids containing d^0 cations and their parents

solid acid	parent oxide	base (pK_a)[a]	ref.
$H_2Ti_4O_9 \cdot H_2O$	$K_2Ti_4O_9$	*n*-alkylamines (9.0)	34
$HNb_3O_8 \cdot H_2O$	KNb_3O_8	*n*-alkylamines (9.0)	35,36
$HTiNbO_5 \cdot H_2O$	$KTiNbO_5$	imidazole (6.95)	37
$HCa_2Nb_3O_{10}$	$CsCa_2Nb_3O_{10}$	3-bromopyridine (2.8)	38,40
$HLaNb_2O_7$	$KLaNb_2O_7$	pyridine (5.3)	39
$H_2La_2Ti_3O_{10}$	$K_2La_2Ti_3O_{10}$	—	41
$HMWO_6 \cdot H_2O$ (M = Nb, Ta)	$LiMWO_6$ (M = Nb, Ta)	quinoxaline (0.56)	42,43
$HMMoO_6 \cdot H_2O$ (M = Nb, Ta)	$LiMMoO_6$ (M = Nb, Ta)	pyrrole (0.4)	44
$H_3PM_{12}O_{40}$ (M = Mo, W)	—	—	45

[a]Corresponds to the lowest pK_a-base that the acid can intercalate.

exchange readily occurs in aqueous acids yielding the corresponding protonated derivatives. A particularly interesting class of such materials are the ion-exchangeable layered perovskites[38–41,46] of the general formulae, $A[A'_{n-1}M_nO_{3n+1}]$ and $A_2[A'_{n-1}M_nO_{3n+1}]$, where A denotes interlayer alkali cations, A′ calcium, lanthanum, *etc*., and M, d^0 cations such as Nb^V and Ti^{IV}. Typical examples are $CsCa_2Nb_3O_{10}$,[38,40] $KLnNb_2O_7$ (Ln = La, Nd)[38,39] and $A_2La_2Ti_3O_{10}$ (A = Na, K),[41] of which the last are Ruddlesden–Popper phases[47] related to $Sr_4Ti_3O_{10}$. In all these cases, the interlayer alkali-metal ions are readily exchanged with protons to yield protonated derivatives. It must be mentioned that first results of ion-exchange in this series were obtained by Tournoux *et al*.,[38] with $ACa_2Nb_3O_{10}$. We show the crystal structures of these oxides in Fig. 6. We see that the MO_6 octahedra are distorted to give short terminal M—O bonds (*ca*. 1.70–1.75 Å) which point to the interlayer region.[38,41] In the protonated derivatives such as $HLnNb_2O_7 \cdot H_2O$ (Ln = La, Nd) and $HCa_2Nb_3O_{10} \cdot 1.5H_2O$, the protons (or H_3O^+ ions) are attached to the short terminal M—O bonds. The strong acidity of the terminal oxygens renders the interlayer protons highly acidic and, accordingly, these materials display Brønsted acidic properties intercalating *n*-alkylamines and other organic bases.[38–40]

An interesting consequence of the distortion of TiO_6 octahedra is seen in the $n = 1$ Ruddlesden–Popper phases

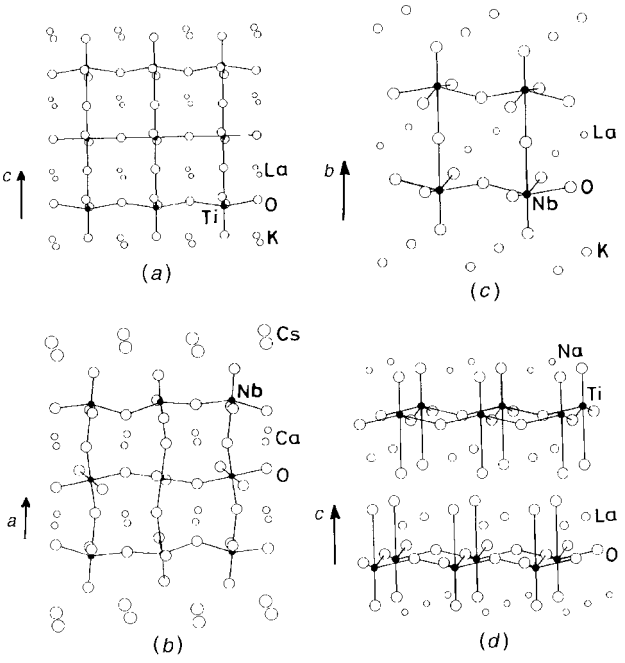

Fig. 6 Structures of layered perovskite oxides: (*a*) $K_2La_2Ti_3O_{10}$, (*b*) $CsCa_2Nb_3O_{10}$, (*c*) $KLaNb_2O_7$ and (*d*) $NaLaTiO_4$

$NaLnTiO_4$ (Ln = lanthanide) originally synthesized by Blasse and Van den Heuvel.[48] The crystal structure of these solids reveals an unique ordering of Na and Ln atoms. Instead of a random distribution of these atoms at the interlayer sites of the parent Sr_2TiO_4 structure, the Na and Ln atoms are ordered in the sequence Na–Na–Ln–Ln··· along the *c*-direction[49] (Fig. 6). This ordering is clearly dictated by the distortion of the TiO_6 octahedra, the oxygens of the short Ti—O bonds pointing towards the Na layer. As a result, the sodium ions are readily ion-exchanged with protons to give another novel series of protonated oxides,[50] $HLnTiO_4 \cdot xH_2O$. It must however be mentioned that an electron microscopic study[51] of the structure of $NaYTiO_4$ revealed the presence of double perovskite layers, $NaTi_2O_7$, separated by [Y—NaO—Y] triple rock-salt layers. Structurally, this phase appears to be closer to $TlBa_2CaCu_2O_7$ than to Ruddlesden–Popper phases.

The Aurivillius family of layered perovskite oxides having the general formula, $(Bi_2O_2)[A_{n-1}M_nO_{3n+1}]$ are a well known series of high-temperature ferroelectric materials, where the distortions of d^0 MO_6 octahedra (M = Ti, Nb, W, *etc*.,) are crucial to the structure, stability and properties.[52–55] Recent crystal structure refinements[56] of representative members of this family, Bi_2WO_6, Bi_3TiNbO_9 and $Bi_4Ti_3O_{12}$, have revealed that cooperative displacements of both the lone-pair Bi^{3+} cations as well as the d^0 cations at the octahedral sites give rise to the observed structures and ferroelectric properties. Interestingly, anion-deficient members of this family having disordered oxygen vacancies around the d^0 cations exhibit high oxide ion conductivities.[57]

$HMM'O_6$ (M = Nb, Ta; M′ = Mo, W) and their hydrates constitute a novel series of layered oxides containing d^0 cations.[42–44] We have synthesized these solids by ion exchange from their lithium analogues, which crystallize in an ordered trirutile structure (Fig. 7) consisting of layers of LiO_6 octahedra alternating with MO_6 and $M'O_6$ octahedra in the *c*-direction.[58] From the structure of $LiNbWO_6$, we see that all the three metal–oxygen octahedra are strongly distorted.[58] Since Li atoms are arranged in sheets perpendicular to the *c*-direction, their removal by exchange with protons in aqueous acids results in a layered structure, in which the short M—O bonds point to the interlayer region where the H_3O^+ ions are located (Fig. 7). Significantly, layered $HMM'O_6$ hydrates are among the strongest solid acids containing MO_6 octahedra, intercalating a variety of organic amines[42,44,59] including weak Lewis bases like 4-nitroaniline ($pK_a = 1.0$), quinoxaline ($pK_a = 0.56$) and pyrrole ($pK_a = 0.4$).

It may be relevant to point out here that the strong Brønsted acidity of heteropoly acids[45] such as $H_3PM_{12}O_{40} \cdot xH_2O$ (M = Mo, W) has its origin in the distorted MO_6 octahedra and the presence of short M—O terminal bonds. The phosphomolybdate anion, $PMo_{12}O_{40}^{3-}$, consists of 12 edge-shared MoO_6 octahedra surrounding a PO_4 tetrahedron. The Mo atoms are displaced towards terminal oxygens giving short (1.70 Å) M—O bonds.[60] The protons and water molecules present in the interconnected space around the heteropolymetallate ions make the solid highly acidic. The phosphomolybdic acids are also fast proton conductors.[61]

Another consequence of the distortion of d^0 MO_6 octahedra is that the M—O bonds are polarized, creating a net dipole moment. When such distorted octahedra are connected up unsymmetrically to give a non-centrosymmetric extended network, the crystal exhibits a macroscopic spontaneous polarization. This polarization is the origin of several ferroic properties[62] which include ferroelectricity and non-linear optical (NLO) behaviour such as second harmonic generation (SHG) of electromagnetic radiation. Typical examples of d^0 oxides showing these properties[63] are $BaTiO_3$, $KNbO_3$, $LiNbO_3$ and $KTiOPO_4$. The ferroic properties of $BaTiO_3$ were first investigated by Merz.[63a] The distortions of MO_6 (M = Ti, Nb) octahedra in ferroelectric perovskites, $BaTiO_3$ and $KNbO_3$, which involve displacement of the M atoms to create one short, two short and three short M—O bonds have been successfully modelled by electronic structure calculations.[22,64] While the calculations clearly show that an admixture (hybridization) between the metal d states and the oxygen 2p states is essential for ferroelectricity, questions relating subtle bonding effects due to A cations on the structure and properties of AMO_3 perovskites (*e.g.* $SrTiO_3$ does not show a ferroelectric transition; $PbTiO_3$ exists in a tetragonal phase that is stable up to 766 K) as well as the relative stabilities of the various ferroelectric phases are yet to be quantitatively understood.

Besides d^0 perovskites, oxides of the general formula, $A_2BM_5O_{15}$, where M is a d^0 cation (such as Nb, Ta together with Mo, W) and A and B are electropositive cations (such as Ba, Na, *etc*.,) exhibit ferroic and non-linear optical properties,[65,66] which are again related to the distortions of d^0 MO_6 octahedra. Oxides of this composition crystallize either with the well known tetragonal tungsten bronze (TTB) structure or with the orthorhombic tungsten bronze (OTB) structure. Typical examples belonging to these structure types are respectively $Ba_2NaNb_5O_{15}$ (banana) and $CsEuNaNb_5O_{15}$, whose ferroic properties are comparable.[65,66]

As we have already mentioned, $LiNbO_3$ and $KTiOPO_4$ (KTP) are among the well known inorganic NLO materials[14,67] whose NLO response could be directly traced to the presence of distorted MO_6 octahedra which are unsymmetrically connected. In KTP the TiO_6 octahedra are connected *cis–trans* creating chains of alternating short (1.70–1.75 Å) and long (2.10–2.15 Å) M—O bonds along the polar axis (Fig. 8). Another structural motif that gives NLO properties among d^0 oxides is the presence of *trans*-connected MO_6 octahedral chains again containing alternate long and short M—O bonds.

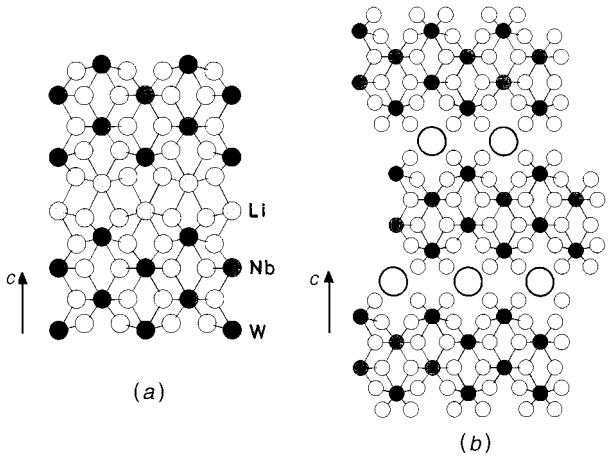

Fig. 7 Schematic structures of (*a*) $LiNbWO_6$ and (*b*) $HNbWO_6 \cdot H_2O$. Open circles around metal atoms denote oxygens. Large open circles in (*b*) denote water molecules.

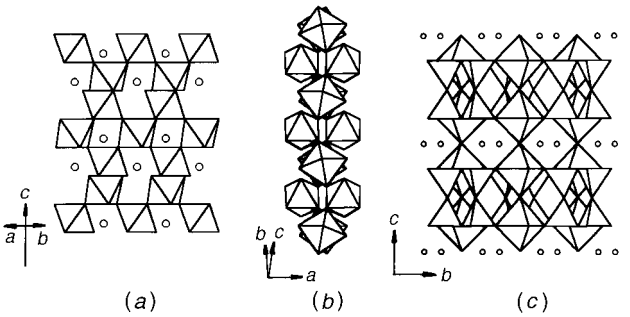

Fig. 8 Structures of (*a*) $LiNbO_3$, (*b*) $KTiOPO_4$ and (*c*) $K_2(NbO)_2Si_4O_{12}$ showing unsymmetrically connected chains of d^0: MO_6 octahedra

Typical examples of this kind of structure are[68,69] $K_2(NbO)_2Si_4O_{12}$ (Fig. 8) and $ANbOB_2O_5$ (A = K, Rb, Cs).

The crucial role of d^0 cations in the NLO properties of KTP-like materials has been revealed[70,71] by synthesizing non-d^0 analogues such as $KSnOPO_4$ and $KSbOSiO_4$, which do not exhibit a significant SHG response. In contrast, considerable substitution of d^0 Nb^V for Ti^{IV} in the KTP structure does not adversely affect the SHG response of $KTiOPO_4$.[72] $LiMM'O_6$ oxides (M = Nb, Ta; M′ = Mo, W) (Fig. 7), crystallizing in a non-centrosymmetric structure ($P\bar{4}2_1m$), show a distinct SHG response that is not destroyed by ion-exchange of lithium by protons.[73] The result clearly reveals that the SHG response of this material is due to the $MM'O_6$ octahedra, the lithium atoms making little contribution to the hyperpolarizability of this material.

Another important property of d^0 oxides is their ability to selectively catalyze oxidation of organic molecules.[12] Selective oxidation of propene to acrolein by bismuth molybdates $[Bi_2Mo_3O_{12}]$[74] and bronzes of the type $[(Bi_2O)Mo_{10}O_{30}]$,[75] and of *n*-butane to maleic anhydride by vanadium phosphates $[VOPO_4/(VO)_2P_2O_7]$[76] are two of the industrially important catalytic conversions, where the role of d^0 cations (Mo^{VI} and V^V) in the catalyst has been established. In recent times, d^0 oxides have been found to exhibit photocatalytic reactivity towards such important reactions as photodecomposition of water[77*a*] and methanol.[77*b*,*c*] Although TiO_2 itself was known for long to split water into hydrogen and oxygen in a photoelectrochemical cell,[78] the use of ion-exchangeable layered perovskites, such as $RbPb_2Nb_3O_{10}$ and $Rb_2La_2Ti_3O_{10}$ as photocatalysts, in these reactions is a significant new development. In addition, $Nd_2Ti_3O_9$, an anion-deficient layered perovskite derived from $K_2Nd_2Ti_3O_{10}$, shows a persistent photoconductivity with a slow decay rate, that appears to be related to oxygen vacancies.[79] Curiously, the recently discovered negative thermal expansion coefficient materials, ZrV_2O_7 and ZrW_2O_8, also contain d^0 cations.[80]

A significant crystal–chemical consequence of the distortions of d^0 MO_6 octahedra is the formation of large period ordered intergrowth structures,[81] as typified by barium siliconiobate–titanates formed between the end members, $Ba_3Nb_6Si_4O_{26}$ and $Ba_3Nb_4Ti_4O_{21}$, and sodium calcium niobates of the general formula $(Na,Ca)_nNb_nO_{3n+2}$. Ordered intergrowth phases are also known among the Aurivillius family of bismuth oxides, $(Bi_2O_2)[A_{n-1}M_nO_{3n+1}]$, between successive members. Typical examples are $Bi_7Ti_4NbO_{21}$ ($n = 2$, 3) and $Bi_9Ti_6CrO_{27}$ ($n = 3$, 4). In all these cases, distorted d^0 MO_6 octahedra play a crucial role in minimizing the elastic strain energy associated with the intergrowth of structurally compatible chemical entities.[81,82]

d^1–d^0 Oxides

A crucial feature of the electronic structure of d^0 oxides is the presence of empty cationic LUMO states which are separated from the filled anionic HOMO states (Fig. 3). Availability of energetically accessible LUMO states renders the d^0 cations in oxides susceptible to reduction.¶ The electron(s) added in the reduction process go to the d-like LUMO states, giving formally a lower oxidation state and a d^n ($0 < n \leqslant 1$, 2 *etc*.,) electronic configuration to the transition metal.[15] Among the large number of such lower valence transition-metal oxides having a partially filled d-shell, those of the early transition metals having a single d electron (d^1, $S = \frac{1}{2}$) are of special attraction. Well known d^1 cations are Ti^{3+}, V^{4+}, Nb^{4+}, Mo^{5+} and W^{5+}. Table 2 lists the representative oxides of these cations together with their significant structural and electronic properties. The list includes not only oxides containing exclusively d^1 cations, but also those having mixed d^1–d^0 configurations. We consider both d^1 and d^1–d^0 oxides together in this article, because they possess certain common features which give useful insights into the evolution of electronic properties.

A significant structural change accompanying the addition of electrons to the LUMO states of d^0 oxides is the suppression of out-of-centre distortion of MO_6 octahedra;[22] the d^1 MO_6 octahedra are invariably more regular than their d^0 MO_6 counterparts. This difference is clearly brought out by comparing the structures, for example, of WO_3 ($5d^0$) and ReO_3($5d^1$) and $BaTiO_3$ ($3d^0$) and $LaTiO_3$ ($3d^1$) (Fig. 9).

From Table 2, we see that early transition-metal oxides containing small d electron counts (d^n: $0 < n \leqslant 1$) exhibit a variety of structural and electronic properties that are distinctly different from the corresponding d^0 oxides. The new properties seem to depend on mainly three factors: (*a*) the principal quantum number of the outer d shell (3d, 4d, or 5d), (*b*) the dimensionality (D) of the crystal structure (3-D, 2-D, 1-D or 0-D) that in turn determines the nature of extended d states formed by hybridization with anionic s/p states and (*c*) the actual details of the crystal structure that determine the nature of metal–oxygen–metal and the metal–metal bonding interactions. Since the nature and energetics of metal d–oxygen s/p orbital interactions are such as to give much broader energy bands with 5d and 4d metals than with 3d metals,[1,15] it is not surprising to find itinerant electron conduction and magnetism with 5d oxides such as ReO_3 and cubic perovskite A_xWO_3 bronzes; rarely if ever we come across localized magnetic spins and magnetic ordering in these materials. With $3d^1$ oxides, on the other hand, we find more often localized electron behaviour and magnetic ordering of spins, a clear signature of narrow band d electrons.

$LaTiO_3$, a prototypical 3d-analogue of ReO_3 and cubic A_xWO_3 bronzes, is a Mott–Hubbard insulator ordering antiferromagnetically[85,105] at $T_N = 120$–150 K. Other $LnTiO_3$ (Ln = lanthanide) oxides are also Mott–Hubbard insulators[106,107] exhibiting fine variations in electronic properties which are attributable to the radius and acidity of Ln^{3+} cations. $LaTiO_3$, $CeTiO_3$ and $PrTiO_3$ seem to belong to one set showing a weakly correlated, antiferromagnetic ordering of d^1 spins, while $GdTiO_3$ and $YbTiO_3$ are strongly correlated ferromagnetic materials; reportedly,[107] $NdTiO_3$ is unique showing no magnetic ordering down to 4.2 K. Hole doping,[108] typically as in $La_{1-x}Sr_xTiO_3$, destroys magnetic ordering and induces metallic behaviour in these systems. None of the hole-doped (d^1–d^0) perovskite titanates however exhibit superconductivity.

The electronic properties of two other titanium(III) oxides, $LiTiO_2$ and $LiTi_2O_4$, stand in marked contrast to those of $LnTiO_3$ perovskites. While $LiTiO_2$ having an ordered rocksalt (hexagonal) structure is metallic and Pauli paramagnetic,[88] $LiTi_2O_4$ having the spinel structure is metallic and superconducting[87] ($T_c = 13$ K). This difference in electronic properties reveals the importance of crystal structure: while the perovskite structure of $LnTiO_3$ which permits linear (*ca.* 180°) Ti—O—Ti interaction leaves the $3d^1$ electron in the π-bonding t_{2g} states, the rocksalt and the spinel structures permit 90° Ti—O—Ti as well as direct Ti—Ti interactions. The difference in electronic properties of perovskite-like $LnTiO_3$ and rocksalt and spinel-type $LiTiO_2$ and $LiTi_2O_4$ could at least be qualitatively understood in terms of the difference in bonding possibilities between the two types of structures. This difference in bonding also points to the futility of looking for direct analogies between d^1 and d^9 perovskite and K_2NiF_4 oxides, in the wake of the discovery of high-temperature superconductivity in copper oxides.[18]

V^{IV} $3d^1$ forms a rich variety of oxides whose properties bring out the influence of structure and dimensionality. While the 3-D cubic perovskite $SrVO_3$ is metallic[91] having no localized moment associated with V^{IV} $3d^1$, the 2-D Sr_2VO_4 (ref. 109)

¶ The ease of reduction depends on the HOMO–LUMO gap. Thus, reducibility of d^0 cations increases as we move from left to right in a period (*e.g.* $TiO_2 < V_2O_5 < CrO_3 < Mn_2O_7$) and from bottom to top in a group (*e.g.* $Ta_2O_5 < Nb_2O_5 < V_2O_5$).

Table 2 d^1 and d^1–d^0 oxides

oxide	characteristic features	ref.
Ti_2O_3	corundum structure; broad metal–insulator (M–I) transition centred around 660 K	15,83
Ti_nO_{2n-1} ($4 \leqslant n \leqslant 9$)	rutile-related crystallographic shear (CS) structures; M–I transitions	15,83
$LnTiO_3$ (Ln = lanthanide)	$GdFeO_3$ structure; electronic property depends on oxygen stoichiometry and Ln. Ln = La: weakly correlated Mott–Hubbard insulator	84–86
$LiTi_2O_4$	spinel structure; superconducting transition at $T_c = 13$ K	87
$LiTiO_2$	ordered rocksalt (hexagonal) structure; metallic and weakly paramagnetic	88
VO_2	rutile-related structure; M–I transition at 340 K	15
V_nO_{2n-1} ($3 \leqslant n \leqslant 10$)	rutile-related CS structure; M–I transitions	83
V_6O_{13}	CS structure derived from V_2O_5	89
$A_xV_2O_5$ (A = Li, Na)	$x = 0.33$: tunnel structure containing highly distorted VO_6 octahedra and VO_5 trigonal bipyramids; possibility of CDW instability and bipolaron ordering	90
$SrVO_3$	perovskite structure; metallic	91
Sr_2VO_4	$n = 1$ R–P[a] phase; semiconducting and antiferromagnetic below 10 K	91
$Sr_3V_2O_7$	$n = 2$ R–P phase; metallic	92
$Sr_4V_3O_{9.7}$	$n = 3$ R–P phase; metallic	93
$(VO_2)P_2O_7$	ladder structure containing double chains of VO_6 octahedra; paramagnetic and insulating	94
$KVOPO_4$	structure contains *cis–trans* bridged VO_6 octahedral chains; paramagnetic insulator	95
NbO_2	distorted rutile structure; semiconductor	96
$Nb_{12}O_{29}$	$3 \times 4 \times \infty$ block structure based on CS of ReO_3 structure; simultaneous metallic conductivity and antiferromagnetic ordering	97
$Rb_2LaNb_2O_7$	$n = 2$ R–P phase; blue–black compound expected to be metallic	98a
Mo_4O_{11} (η and γ)	two-dimensional structure consisting of three octahedra thick ReO_3 slabs bridged by MoO_4 tetrahedra; CDW instability	17
Mo_nO_{3n-1} ($n = 8, 9$)	ReO_3-related CS structure based on {102}; CDW instability	99
$A_{0.30}MoO_3$ (A = K, Rb, Tl)	'blue' bronzes; one-dimensional structure containing clusters of MoO_6 octahedra; CDW instability	17,99
$A_{0.33}MoO_3$ (A = K, Rb, Cs, Tl)	'red' bronzes; one-dimensional structure consisting of clusters of six MoO_6 octahedra; semiconductors	17
$A_{0.9}Mo_6O_{17}$ (A = Li, Na, K)	'purple' bronzes; layered structure consisting of four octahedra-thick MoO_6 slabs bridged by MoO_4 tetrahedra; CDW instability; the lithium compound shows a superconducting transition at $T_c = 1.9$ K	17,99
WO_{3-x} ($0 < x \leqslant 0.11$)	CS phases based on {102} and {103} on ReO_3 structure; semiconducting	100
$W_{18}O_{49}$	tunnel structure containing pentagonal columns; metallic	100
A_xWO_3 (A = electropositive metal)	structure and properties depend on A and x; for alkali metals and $x > 0.3$, metallic behaviour	101,102
$(PO_2)_4(WO_3)_{2m}$ ($2 \leqslant m \leqslant 14$)	monophosphate tungsten bronzes with pentagonal tunnels; quasi low-dimensional structures isotypic with orthorhombic Mo_4O_{11}; $m = 4$ and 6 members show distinct CDW instability	103
ReO_3	cubic perovskite; metallic	15,104

[a]Ruddlesden–Popper.

having the K_2NiF_4 structure [$n = 1$ member of the Ruddlesden–Popper (R–P) series], is semiconducting and antiferromagnetic below 10 K. $Sr_3V_2O_7$ (ref. 92*a*) and $Sr_4V_3O_{9.7}$ (ref. 93, 110) ($n = 2$ and $n = 3$ members of the R–P series) are metallic down to 4.2 K. While the effect of dimensionality on the electronic properties of these d^1 oxides is obvious, there seems to be a correlation between the degree of distortion of the VO_6 octahedra and the electronic properties.[110] For this purpose, the degree of distortion is expressed as $[(V-O)_{apical} - (V-O)_{planar}]/(V-O)_{planar}$. For metallic $SrVO_3$, the distortion is exactly zero since all the six V—O bond lengths (1.92 Å) are equal. For semiconducting Sr_2VO_4 which has elongated VO_6 octahedra with four planar V—O bonds at 1.917 Å and the two apical V—O bonds at 1.986 Å, the degree of distortion is 0.036. For the metallic $Sr_4V_3O_{9.7}$, there are two kinds of VO_6 octahedra, the terminal and the central;

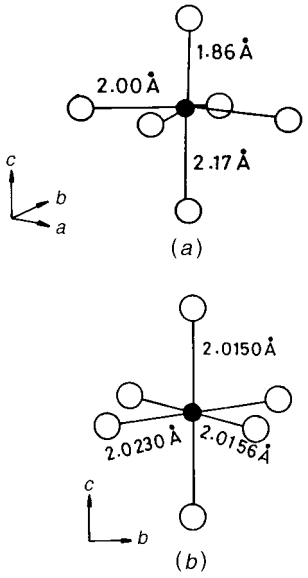

Fig. 9 TiO_6 octahedra in (*a*) ferroelectric $BaTiO_3$ and (*b*) $LaTiO_3$

the distortion indices are, respectively, 0.021 and 0.004, suggesting that the d electrons of the central octahedra are delocalized and those of terminal octahedra are localized. Magnetic susceptibility data lend support to this possibility. Similar correlation between the degree of distortion and electronic properties seems to exist in $LnTiO_3$ perovskites.[110]

It is interesting to compare the distortion of VO_6 octahedra in two other vanadium(IV) oxides, $(VO)_2P_2O_7$ (ref. 94) (Fig. 10) and $KVOPO_4$ (ref. 95). $(VO)_2P_2O_7$ possesses 1-D double-chains of VO_6 octahedra which are linked by P_2O_7 groups, while $KVOPO_4$ adopts the KTP structure (Fig. 8) containing unsymmetrically connected chains of VO_6 octahedra. In both the structures, the VO_6 octahedra are considerably distorted, the metal atom moving away from the centre, indicating that for low-dimensional vanadium(IV) oxides which are insulating, the out-of-centre distortion of VO_6 octahedra persists even for d^1 electronic configuration.

Oxides containing $4d^1$ NbO_6 octahedra are less numerous. Rutile-like NbO_2[96] exhibiting semiconducting behaviour is similar to VO_2, where the $4d^1$ electrons of NbO_6 octahedra are tied into metal–metal bonds across the edge-shared octahedra of the rutile structure. Among the binary oxides containing Nb^{IV}, $Nb_{12}O_{29}$ is well characterized.[97] It has a $3\times4\times\infty$ block structure (Fig. 11) consisting of pillars of ReO_3

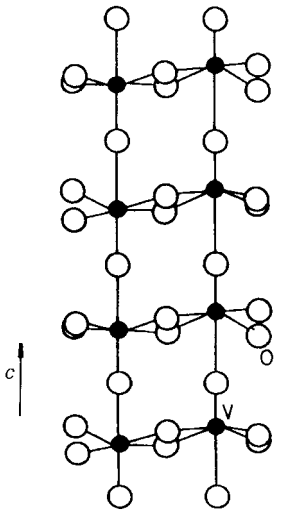

Fig. 10 Structure of $(VO)_2P_2O_7$. For clarity, P atoms are not shown.

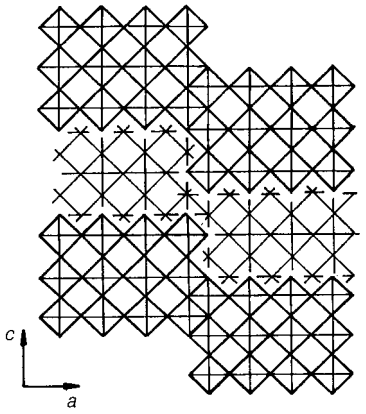

Fig. 11 Structure of $Nb_{12}O_{29}$

structure bridged by edge-sharing octahedra at the pillar boundaries. This oxide is unique in that it is an itinerant electron antiferromagnet exhibiting both metallic conductivity and antiferromagnetic ordering at 12 K. While there are no definite perovskite-type niobium(IV) oxides known at present, an $n=2$ member of the R–P phase, $Rb_2LaNb_2O_7$, has been reported.[98a] Its electronic property is not known, but extended Hückel calculations predict 2-D metallic properties for this material. It has however been reported recently[98b] that a lithium-intercalated layered perovskite, $KCa_2Nb_3O_{10}$, exhibits a superconducting transition around 1 K.

Unlike niobium, molybdenum forms a variety of oxides where the electronic configuration of the metal is $4d^1$–$4d^0$. $LnMoO_4$ (Ln = Gd–Lu, Y) oxides[111] are unique among them in that they contain isolated tetrahedral MoO_4^{3-} ions in the scheelite structure. The cubic tungsten bronze analogues of molybdenum, A_xMoO_3 (A = Na, K; $x\approx0.90$–0.97), which are prepared under high (65 kbar) pressure,[112] are metastable under ordinary pressure and temperatures. These materials are similar to the cubic tungsten bronzes, showing metallic behaviour without spontaneous magnetism.

Under ordinary pressures, molybdenum forms several novel quasi-low-dimensional oxides and oxide bronzes containing 4d electrons.[17,99] These materials have attracted considerable attention during the last decade in view of the unique low-dimensional electronic properties which include CDW driven metal–insulator transitions, sliding CDWs and insulator–superconductor transitions.

CDW and superconductivity are two most fascinating properties exhibited by a number of low-dimensional transition-metal compounds having small d electron counts.[113] Both the phenomena arise from a common origin, namely strong electron–phonon interaction. The possibility of a CDW accompanied by a lattice distortion was first predicted by Peierls[114] and Fröhlich[115] for a 1-D metal. The distortion and the associated electronic transition arise from a coupling of conduction electrons and phonons at $2K_F$ (where K_F is the Fermi wavevector corresponding to the reciprocal unit cell dimension); the coupling leads to a spontaneous lattice distortion and a modulation of the charge density (hence the name CDW) at $T>0$ K, if the gain in electronic energy due to opening of a gap at the Fermi surface is greater than the potential energy cost of the lattice distortion. In a strictly 1-D metal, the gap opening is complete and the transition is a clean metal–non-metal (Peierls) transition. For quasi-low-dimensional systems, the CDW transition is associated with partial gap openings at the Fermi surface and therefore one finds metal–metal transitions rather than metal–non-metal transitions.

CDW was first experimentally realized[116] in the niobium and tantalum chalcogenides such as $NbSe_3$, TaS_2 and $TaSe_2$. When CDW was discovered in the blue molybdenum

bronze,[117] $K_{0.3}MoO_3$ which is chemically and structurally different from the niobium and tantalum chalcogenides, it gave rise to considerable excitement and impetus to the study of low-dimensional molybdenum oxides and bronzes. Investigations over the last decade have established the occurrence of CDW and related electronic properties in at least three distinct types of molybdenum oxides: the blue bronzes, $A_{0.3}MoO_3$, the purple bronzes, $A_{0.9}Mo_6O_{17}$ and Mo_nO_{3n-1} oxides. Since these developments have been authoritatively discussed in the literature,[17,99] we recount only the salient features here.

Among the three structure types of molybdenum oxides which exhibit CDW related instabilities, the blue molybdenum bronzes, $A_{0.3}MoO_3$ (A = K, Rb and Tl) possess essentially a 1-D structure (Fig. 12) consisting of clusters of ten edge-sharing MoO_6 octahedra linked by corners. A complete study of the structure and properties of the blue bronze, $Tl_{0.3}MoO_3$, has been carried out by Ganne *et al.*[118] The purple bronzes, $A_{0.9}Mo_6O_{17}$ (A = Na, K, Tl), of which the potassium compound is prototypical, crystallize in a layered structure consisting of four sheets of ReO_3-like MoO_6 octahedra which are capped by corner-sharing MoO_4 tetrahedra (Fig. 12). The potassium atoms are located in the interlayer positions. While the effective valence of tetrahedral-site molybdenum is 6+, the valences of octahedral-site molybdenums are 5.1+ and 5.8+ for the two crystallographically non-equivalent molybdenum atoms. The purple molybdenum bronze, $TlMo_6O_{17}$, exhibiting a Peierls distortion at 120 K, is truly stoichiometric whose structure has been accurately refined ($R = 0.02$) in the space group $P\bar{3}m1$ (ref. 119). The effective valence of the tetrahedral site molybdenum is 5.9+, while the valences of the octahedral site molybdenums are 5.0+ and 5.6+ in this compound. Clearly, the central molybdenum atoms carry the majority of the 4d electrons in the 2-D structure. A purple bronze is also known for lithium, $Li_{0.9}Mo_6O_{17}$, whose structure is slightly different.[17]

The structure of Mo_4O_{11} (Fig. 12) is closely related to that of the purple bronzes. Mo_4O_{11} which was first synthesized by Kihlborg[120] exists in two structural modifications, the low-temperature η form is monoclinic and the high-temperature γ form is orthorhombic. Both the structures consist of corner-sharing three octahedra thick MoO_6 slabs which are interconnected by MoO_4 tetrahedra. While the valency of tetrahedral molybdenum is 6+ as expected, the valencies of the three octahedral molybdenum atoms are 5.85+, 5.40+ and 5.02+, revealing that the 4d electrons are essentially confined in the two-dimensional slabs. While the adjacent slabs are identical in the monoclinic Mo_4O_{11}, they are mirror images in the orthorhombic Mo_4O_{11}. Another difference between the two structures is that the tunnels between adjacent slabs are pentagonal in the orthorhombic phase and they are hexagonal in the monoclinic phase.

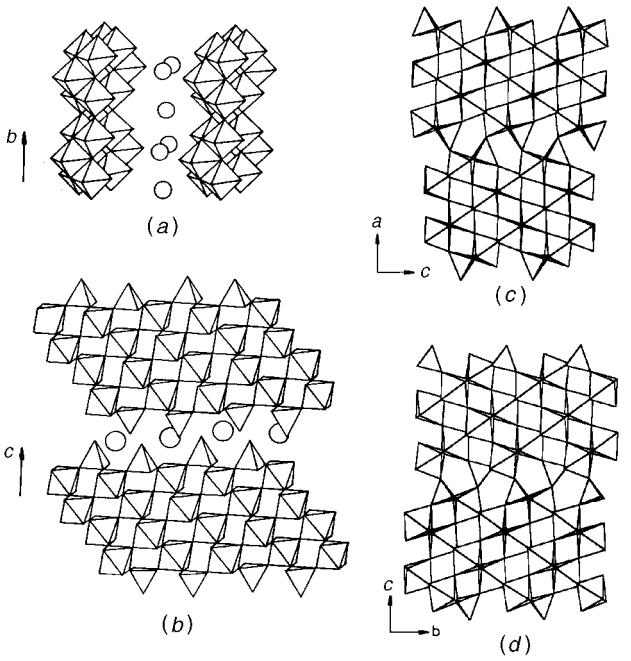

Fig. 12 Structures of (*a*) 'blue' bronze, $K_{0.3}MoO_3$, (*b*) 'purple' bronze, $K_{0.9}Mo_6O_{17}$, (*c*) orthorhombic Mo_4O_{11} and (*d*) monophosphate tungsten bronze, $(PO_2)_4(WO_3)_m$, $m = 6$ member

All the three types of molybdenum oxides exhibit CDW instabilities and the associated low-dimensional electronic properties at low temperatures.[17,99] The occurrence of underlying lattice distortions and nesting of Fermi surfaces through CDW transition have been clearly established in all the cases. Among these oxides, the purple bronze of lithium, $Li_{0.9}Mo_6O_{17}$, is unique showing a superconducting transition at $T_c \approx 1.9$ K in addition to a sharp increase in resistivity at 24 K.[17,99]

Among the other oxides of molybdenum containing 4d electrons, the red bronzes $A_{0.33}MoO_3$ (A = K,Rb,Cs,Tl) are characteristically different, showing only a semiconducting behaviour.[17] The structural origin of the semiconducting properties of the red molybdenum bronzes has been established by band-structure calculations.[121] Crystallographic shear phases of the general formula, Mo_nO_{3n-1} ($n = 8, 9, 10$) originally synthesized by Magnéli and co-workers[122] also exhibit anisotropic electrical transport and other properties characteristic of CDW transition between 100 and 200 K.[99]

While the unmistakable link between electronic instability (due to coupling of conduction electrons and phonons) and the quasi-low-dimensional structure in these molybdenum oxides is well established, what is intriguing from the solid state chemistry standpoint is that whether the CDW and related phenomena are something special only to the quasi-low-dimensional molybdenum oxides containing delocalized 4d electrons or the phenomena are much more general involving other d^1 systems as well. In this context, we focus attention on to the discovery[103] of CDW-driven electronic instabilities in phosphate tungsten bronzes of the general formula, $(PO_2)_4(WO_3)_{2m}$. The structures of these materials (Fig. 12), originally synthesized by Raveau and co-workers,[123] consists of ReO_3-like slabs of corner-shared WO_6 octahedra connected by PO_4 tetrahedra forming layers in the *ab*-plane of the orthorhombic unit cell. As such, the structures of these materials are similar to those of Mo_4O_{11}, the PO_4 tetrahedra replacing MoO_4 tetrahedra and WO_6 octahedra replacing MoO_6 octahedra in the latter. Indeed, there are two kinds of monophosphate tungsten bronzes, one with pentagonal tunnels and the other with hexagonal tunnels, respectively being isostructural with the orthorhombic and monoclinic modifications of Mo_4O_{11}.[1] While the $m = 2$ member, $P_2W_2O_{10}$, shows a high anisotropic electrical conductivity that is semiconductor-like in the range 10–390 K, the $m = 4$ and 6 members show metallic behaviour with giant anomalies between 60 and 115 K suggesting unmistakable CDW instabilities, which are further substantiated by X-ray diffuse scattering studies and band structure calculations.[103] These results unambiguously reveal that confinement of 5d electrons of WO_6 octahedra in 2-D structures can give rise to structural and electronic instabilities similar to those of molybdenum bronzes and oxides containing 4d electrons.

Conclusion

The brief survey of early transition metal oxides containing d^0 and d^1–d^0 electronic configurations reveals an intimate relationship between the crystal structure and electronic properties. The characteristic out-of-centre distortion of metal–oxygen (MO_6) octahedra in many d^0 oxides is at the heart of several of the interesting properties, including formation of

layered structures exhibiting ion-exchange and intercalation, Brønsted acidity, ferroelectric and non-linear optical response. Oxides containing d^1 MO_6 octahedra exhibit a variety of electrical and magnetic properties that owe their origin to the nature of d-like states near the Fermi level. While $5d^1$ and $4d^1$ electrons in three-dimensional (3-D) structures give rise to itinerant electron magnetism and conduction, $3d^1$ electrons in low-dimensional structures are localized. The properties of $3d^1$ titanium(III) oxides possessing perovskite, rocksalt and spinel structures show an interesting correlation with crystal structure and bonding that reveals the futility of looking for d^1 analogues of superconducting cuprates. Molybdenum oxides and bronzes containing 4d electrons, which are confined to low-dimensional structures, exhibit characteristic CDW-driven electronic instabilities arising from a strong electron–phonon interaction. Recent investigations reveal that similar instabilities can be induced in low-dimensional tungsten oxides containing 5d electrons.

The authors thank the Indo–French Centre for the Promotion of Advanced Research, New Delhi for financial support. The authors also would like to thank one of the reviewers of this manuscript for drawing our attention to some of the significant works on d^0 and d^1/d^0 oxides.

References

1 (*a*) C. N. R. Rao and B. Raveau, *Transition Metal Oxides*, VCH Publishers, New York, 1995; (*b*) P. A. Cox, *Transition Metal Oxides: An Introduction to their Electronic Structure and Properties*, Clarendon, Oxford, 1992.
2 A. D. Wadsley in *Non-stoichiometric Compounds*, ed. L. Mandelcorn, Academic Press, New York, 1964, p. 98.
3 *Solid State Chemistry*, ed. R. S. Roth and S. J. Schneider Jr., NBS Special Publication 364, National Bureau of Standards, Washington DC, 1972.
4 A. F. Wells, *Structural Inorganic Chemistry*, 5th edn., Clarendon Press, Oxford, 1984.
5 F. Hulliger, *Structural Chemistry of Layer-Type Phases*, ed. F. Levy, D. Reidel Publishing Company, Dordrecht, 1976.
6 L. A. Bursill, B. G. Hyde and M. O'Keeffe, in ref. 3, p. 197.
7 C. R. A. Catlow and R. James, in *Chemical Physics of Solids and their Surfaces*, The Royal Society of Chemistry, London, 1980, vol. 8, pp. 108–120.
8 P. Hagenmuller, *Prog. Solid State Chem*., 1971, **5**, 71.
9 A Magnéli, *Pure Appl. Chem*., 1978, **50**, 1261.
10 J. S. Anderson and R. J. D. Tilley, in *Surface and Defect Properties of Solids*, The Chemical Society, London, 1974, vol. 3, p. 1.
11 A. Corma, *Chem. Rev*., 1995, **95**, 559.
12 *Solid State Chemistry in Catalysis*, ed. R. K. Graselli and J. F. Brazdil, ACS Symp. Ser. 279, American Chemical Society, Washington DC, 1985.
13 Y-W Liou and C. M. Wang, *J. Electrochem. Soc*., 1996, **143**, 1492.
14 D. F. Eaton, *Science*, 1991, **253**, 281.
15 J. B. Goodenough, *Prog. Solid State Chem*., 1971, **5**, 145.
16 P. P. Edwards, T. V. Ramakrishnan and C. N. R. Rao, *J. Phys. Chem*., 1995, **99**, 5228.
17 *Low-Dimensional Electronic Properties of Molybdenum Bronzes and Oxides*, ed. C. Schlenker, Kluwer, Dordrecht, 1989.
18 A. W. Sleight, *Science*, 1988, **242**, 1519.
19 M. Kunz and I. D. Brown, *J. Solid State Chem*., 1995, **115**, 395.
20 Ref. 5, p. 181.
21 Ref. 4, p. 1198.
22 R. A. Wheeler, M. H. Whangbo, T. Hughbanks, R. Hoffmann, J. K. Burdett and T. A. Albright, *J. Am. Chem. Soc*., 1986, **108**, 2222.
23 S. K. Kang, H. Tang and T. A. Albright, *J. Am. Chem. Soc*., 1993, **115**, 1971.
24 (*a*) R. G. Pearson, *Chem. Br*., 1967, **3**, 103; (*b*) J. E. Huheey, *Inorganic Chemistry*, 3rd edn., Harper International Edition, Cambridge, 1983, pp. 312–325.
25 J. T. Szymanski and A. C. Roberts, *Can. Mineral*., 1984, **22**, 681.
26 (*a*) B. Krebs, A. Müller and H. Beyer, *Inorg. Chem*., 1969, **8**, 436; (*b*) H. Beyer, O. Glemser and B. Krebs, *Angew. Chem., Int. Ed. Engl*., 1968, **7**, 295.
27 (*a*) J. M. Longo and P. Kierkegaard, *Acta Chem. Scand*., 1996, **20**, 72; (*b*) J. M. Longo, J. W. Pierce and J. A. Kafalas, *Mater. Res. Bull*., 1971, **6**, 1157.
28 M. Tachez, F. Theobald, J. Bernard and A. W. Hewat, *Rev. Chim. Miner*., 1982, **19**, 291.
29 K. Beneke and G. Lagaly, *Inorg. Chem*., 1983, **22**, 1503.
30 (*a*) N. S. P. Bhuvanesh and J. Gopalakrishnan, unpublished work; (*b*) N. S. P. Bhuvanesh, Ph. D. Thesis, Indian Institute of Science, 1997.
31 A. L. Garcia-Ponce, L. Moreno-Real and A. J. Lopez, *J. Solid State Chem*., 1990, **87**, 20.
32 (*a*) B. Krebs, *Acta Crystallogr, Sect. B*, 1972, **28**, 2222; (*b*) N. Boudjada, J. Rodriguez-Carvajal, M. Anne and M. Figlarz, *J. Solid State Chem*., 1993, **105**, 211.
33 S. Åsbrink and B. G. Brandt, *Chem. Scr*., 1971, **1**, 169.
34 P. Clement and R. Marchand, *C. R. Acad. Sci. Paris*, 1983, **296**, 1161.
35 R. Nedjar, M. M. Borel and B. Raveau, *Mater. Res. Bull*., 1985, **20**, 1291.
36 R. Nedjar, M. M. Borel and B. Raveau, *Z. Anorg. Allg. Chem*., 1986, **540/541**, 198.
37 H. Rebbah, G. Desgardin and B. Raveau, *Mater. Res. Bull*., 1979, **14**, 1125.
38 (*a*) M. Dion, M. Ganne and M. Tournoux, *Mater. Res. Bull*., 1981, **16**, 1429; (*b*) M. Dion, M. Ganne, M. Tournoux and J. Ravez, *Rev. Chim. Miner*., 1984, **21**, 92; (*c*) M. Dion, M. Ganne and M. Tournoux, *Rev. Chim. Miner*., 1986, **23**, 61.
39 J. Gopalakrishnan, V. Bhat and B. Raveau, *Mater. Res. Bull*., 1987, **22**, 413.
40 (*a*) A. J. Jacobson, J. T. Lewandowski and J. W. Johnson, *J. Less-Common Metals*, 1986, **116**, 137; (*b*) A. J. Jacobson, J. W. Johnson and J. T. Lewandowski, *Mater. Res. Bull*., 1987, **22**, 45.
41 (*a*) J. Gopalakrishnan and V. Bhat, *Inorg. Chem*., 1987, **26**, 4299; (*b*) M. Richard, L. Brohan and M. Tournoux, *J. Solid State Chem*., 1994, **112**, 345; (*c*) A. J. Wright and C. Greaves, *J. Mater. Chem*., 1996, **6**, 1823.
42 V. Bhat and J. Gopalakrishnan, *Solid State Ionics*., 1988, **26**, 25.
43 N. Kumada, M. Takeshita, F. Muto and N. Kinomura, *Mater. Res. Bull*., 1988, **23**, 1053.
44 N. S. P. Bhuvanesh and J. Gopalakrishnan, *Inorg. Chem*., 1995, **34**, 3760.
45 J. B. Goodenough, in *Chemistry and Uses of Molybdenum*, ed. H. F. Barry and P. C. H. Mitchell, Climax Molybdenum Company, Ann Arbor, Michigan, 1982, p. 17.
46 J. Gopalakrishnan, *Chem. Mater*., 1995, **7**, 1265.
47 (*a*) S. N. Ruddlesden and P. Popper, *Acta Crystallogr*., 1957, **10**, 538; (*b*) S. N. Ruddlesden and P. Popper, *Acta Crystallogr*., 1958, **11**, 54.
48 (*a*) G. Blasse, *J. Inorg. Nucl. Chem*., 1968, **30**, 656; (*b*) G. Blasse and G. P. M. Van den Heuvel, *J. Solid State Chem*., 1974, **10**, 206.
49 (*a*) K. Toda, Y. Kameo, M. Ohta and M. Sato, *J. Alloys Compd*., 1995, **218**, 228; (*b*) S-H. Byeon, K. Park and M. Itoh, *J. Solid State Chem*., 1996, **121**, 430.
50 S-H. Byeon, J. J. Yoon and S. O. Lee, *J. Solid State Chem*., 1996, **127**, 119.
51 M. Richard, G. Goglio and L. Brohan, *Mater. Res. Bull*., 1995, **30**, 925.
52 (*a*) B. Aurivillius, *Ark. Kemi*, 1949, **1**, 463; (*b*) B. Aurivillius, *Ark. Kemi*, 1951, **2**, 519.
53 R. E. Newnham, R. W. Wolfe and J. F. Dorrian, *Mater. Res. Bull*., 1971, **6**, 1029.
54 A. Ramanan, J. Gopalakrishnan and C. N. R. Rao, *J. Solid State Chem*., 1985, **60**, 376.
55 B. Frit and J. P. Mercurio, *J. Alloys Compd*., 1992, **188**, 27.
56 R. L. Withers, J. G. Thompson and A. D. Rae, *J. Solid State Chem*., 1991, **94**, 404.
57 (*a*) F. Abraham, M. F. Debreuille-Gresse, G. Mairesse and G. Nowogrocki, *Solid State Ionics*., 1988, **28–30**, 529; (*b*) K. R. Kendall, C. Navas, J. K. Thomas and H-C. zur Loye, *Chem. Mater*., 1996, **8**, 642.
58 J. L. Fourquet, A. Le Bail and P. A. Gillet, *Mater. Res. Bull*., 1988, **23**, 1163.
59 N. Kinomura and N. Kumada, *Solid State Ionics*., 1992, **51**, 1.
60 Ref. 4, pp. 520–523.
61 A. Clearfield, *Chem. Rev*., 1988, **88**, 142.
62 R. E. Newnham, *Structure–Property Relations*, Springer-Verlag, New York, 1975.
63 (*a*) W. J. Merz, *Phys. Rev*., 1949, **76**, 1221; (*b*) J. B. Goodenough and J. M. Longo, *Landolt-Börnstein Numerical Data and Functional Relationships in Science and Technology*, *New Series, Group III*, ed. K. H. Hellwege, Springer-Verlag, Berlin, 1970, vol. 4a.

64 R. E. Cohen, *Nature* (*London*), 1992, **358**, 136.
65 See, for example: P. Hagenmuller, *Proc. Indian Acad. Sci.* (*Chem. Sci.*), 1983, **92**, 1.
66 (*a*) M. Tournoux, M. Ganne and Y. Piffard, *J. Solid State Chem.*, 1992, **96**, 141; (*b*) M. Dion, M. Ganne, M. Tournoux and J. Ravez, *J. Solid State Chem.*, 1984, **53**, 422.
67 J. D. Bierlein and H. Vanherzeele, *J. Opt. Soc. Am. B*, 1989, **6**, 622.
68 M. P. Crosnier, D. Guyomard, A. Verbaere, Y. Piffard and M. Tournoux, *J. Solid State Chem.*, 1992, **98**, 128.
69 A. Akella and D. A. Keszler, *J. Solid State Chem.*, 1995, **120**, 74.
70 P. A. Thomas, A. M. Glazer and B. E. Watts, *Acta Crystallogr., Sect. B*, 1990, **46**, 333.
71 M. P. Crosnier, D. Guyomard, A. Verbaere and Y. Piffard, *Eur. J. Solid State Inorg. Chem.*, 1990, **27**, 845.
72 K. K. Rangan, B. R. Prasad, C. K. Subramanian and J. Gopalakrishnan, *J. Chem. Soc., Chem. Commun.*, 1994, 141.
73 N. S. P. Bhuvanesh, B. R. Prasad, C. K. Subramanian and J. Gopalakrishnan, *Chem. Commun.*, 1996, 289.
74 A. W. Sleight, *Science*, 1980, **208**, 895.
75 M. Forissier, N. G. Ching Fai, M. Ganne and M. Tournoux, *Bull. Soc. Chim. Fr.*, 1989, 745.
76 G. Centi, F. Trifiro, J. R. Ebner and V. M. Franchetti, *Chem. Rev.*, 1988, **88**, 55.
77 (*a*) T. Takata, Y. Furumi, K. Shinohara, A. Tanaka, M. Hara, J. N. Kondo and K. Domen, *Chem. Mater.*, 1997, **9**, 1063; (*b*) J. Yoshimura, Y. Ebina, J. Kondo, K. Domen and A. Tanaka, *J. Phys. Chem.*, 1993, **97**, 1970; (*c*) Y-W. Liou and C. M. Wang, *J. Electrochem. Soc.*, 1996, **143**, 1492.
78 A. Fujishima and K. Honda, *Nature* (*London*), 1972, **238**, 37.
79 B. Dulieu, J. Bullot, J. Wery, M. Richard and L. Brohan, *Phys. Rev. B*, 1996, **53**, 10 641.
80 (*a*) A. W. Sleight, *Endeavour*, 1995, **19**, 64; (*b*) T. A. Mary, J. S. O. Evans, T. Vogt and A. W. Sleight, *Science*, 1996, **272**, 90.
81 R. J. D. Tilley, in *Chemical Physics of Solids and their Surfaces*, The Royal Society of Chemistry, London, 1980, vol. 8, pp. 149–160 and references therein.
82 C. N. R. Rao and J. M. Thomas, *Acc. Chem. Res.*, 1985, **18**, 113.
83 J. M. Honig and L. L. Van Zandt, *Annu. Rev. Mater. Sci.*, 1975, **5**, 225.
84 D. A. MacLean, H-N. Ng and J. E. Greedan, *J. Solid State Chem.*, 1979, **30**, 35.
85 F. Lichtenberg, D. Widmer, J. G. Bednorz, T. Williams and A. Reller, *Z. Phys. B: Condens. Matter*, 1991, **82**, 211.
86 C. Eylem, G. Saghi-Szabo, B.-H. Chen, B. Eichhorn, J.-L. Peng, R. L. Greene, L. Salamanca-Riba and S. Nahm, *Chem. Mater.*, 1992, **4**, 1038.
87 D. C. Johnston, H. Prakash, W. H. Zachariasen and R. Viswanathan, *Mater. Res. Bull.*, 1973, **8**, 777.
88 T. A. Hewston and B. L. Chamberland, *J. Phys. Chem. Solids*, 1987, **48**, 97.
89 D. W. Murphy and P. A. Christian, *Science*, 1979, **205**, 651.
90 M. Greenblatt in ref. 17, p. 1.
91 (*a*) M. J. Rey, Ph. Dehaudt, J. C. Joubert, B. Lambert-Andron, M. Cyrot and F. Cyrot-Lackmann, *J. Solid State Chem.*, 1990, **86**, 101; (*b*) T. Palanisamy, J. Gopalakrishnan and M. V. C. Sastri, *Z. Anorg. Allg. Chem.*, 1975, **415**, 275.
92 (*a*) A. Nozaki, H. Yoshikawa, T. Wada, H. Yamauchi and S. Tanaka, *Phys. Rev. B*, 1991, **43**, 181; (*b*) N. Suzuki, T. Noritake, N. Yamamota and T. Hiroki, *Mater. Res. Bull.*, 1991, **26**, 1.
93 M. Itoh, M. Shikano, R. Liang, H. Kawaji and T. Nakamura, *J. Solid State Chem.*, 1990, **88**, 597.
94 D. C. Johnston, J. W. Johnson, D. P. Goshorn and A. J. Jacobson, *Phys. Rev. B*, 1987, **35**, 219.
95 M. L. F. Phillips, W. T. A. Harrison, T. E. Gier, G. D. Stucky, G. V. Kulkarni and J. K. Burdett, *Inorg. Chem.*, 1990, **29**, 2158.
96 (*a*) D. B. Rogers, R. D. Shannon, A. W. Sleight and J. L. Gillson, *Inorg. Chem.*, 1969, **8**, 841; (*b*) A. K. Cheetham and C. N. R. Rao, *Acta Crystallogr., Sect. B*, 1976, **32**, 1579.
97 R. J. Cava, B. Batlogg, J. J. Krajewski, P. Gammel, H. F. Poulson, W. F. Peck Jr. and L. W. Rupp Jr., *Nature* (*London*), 1991, **350**, 598.
98 (*a*) A. R. Armstrong and P. A. Anderson, *Inorg. Chem.*, 1994, **33**, 4366; (*b*) Y. Takano, S. Takayanagi, S. Ogawa, T. Yamadaya and N. Mori, Technical Report A. 3245 from The Institute for Solid State Physics, The University of Tokyo, Japan, 1997.
99 M. Greenblatt, *Chem. Rev.*, 1988, **88**, 31.
100 W. Sahle, *Chem. Commun., Univ. Stockholm*, 1993.
101 T. Ekström and R. J. D. Tilley, *Chem. Scr.*, 1980, **16**, 1.
102 P. Hagenmuller, in *Comprehensive Inorganic Chemistry*, ed. J. C. Bailer, H. J. Emeleus, R. Nyholm and A. F. T. Dickenson, Pergamon, Oxford, 1973, vol. 4.
103 M. Greenblatt, *Acc. Chem. Res.*, 1996, **29**, 219.
104 C. N. R. Rao, *Annu. Rev. Phys. Chem.*, 1989, **40**, 291.
105 D. A. Crandles, T. Timusk and J. E. Greedan, *Phys. Rev. B*, 1991, **44**, 13250.
106 H. L. Ju, C. Eylem, J. L. Peng, B. W. Eichhorn and R. L. Greene, *Phys. Rev. B*, 1994, **49**, 13335.
107 D. A. MacLean, K. Sato and J. E. Greedan, *J. Solid State Chem.*, 1980, **40**, 241.
108 Y. Tokura, Y. Taguchi, Y. Okada, Y. Fujishima, T. Arima, K. Kumagai and Y. Iye, *Phys. Rev. Lett.*, 1993, **70**, 2126.
109 M. Cyrot, B. Lambert-Andron, J. L. Soubeyroux, M. J. Rey, Ph. Dehauht, F. Cyrot-Lackmann, G. Fourcaudiot, J. Beille and J. L. Tholence, *J. Solid State Chem.*, 1990, **85**, 321.
110 W. Gong, J. S. Xue and J. E. Greedan, *J. Solid State Chem.*, 1991, **91**, 180.
111 E. Banks and M. Nemiroff, *Inorg. Chem.*, 1974, **11**, 2715.
112 T. A. Bither, J. L. Gillson and H. S. Young, *Inorg. Chem.*, 1966, **5**, 1559.
113 See, for example: (*a*) R. H. Friend and A. D. Yoffe, *Adv. Phys.*, 1987, **36**, 1; (*b*) E. Canadell and M. H. Whangbo, *Chem. Rev.*, 1991, **91**, 965 and references therein.
114 R. E. Peierls, *Quantum Theory of Solids*, Clarendon, Oxford, 1955, p. 108.
115 H. Fröhlich, *Proc. R. Soc. London, Ser. A*, 1954, **223**, 296.
116 (*a*) P. Monceau, N. P. Ong, A. M. Portis, A. Meerschaut and J. Rouxel, *Phys. Rev. Lett.*, 1976, **37**, 602; (*b*) F. J. Di Salvo and T. M. Rice, *Phys. Today*, April 1979, 32; (*c*) *Crystal Chemistry and Properties of Materials with Quasi-One-Dimensional Structures*, ed. J. Rouxel, D. Reidel, Dordrecht, 1986.
117 R. Buder, J. Devenyi, J. Dumas, J. Marcus, J. Mercier, C. Schlenker and H. Vincent, *J. Phys. Lett.*, 1982, **43**, L59.
118 M. Ganne, A. Boumaza, M. Dion and J. Dumas, *Mater. Res. Bull.*, 1985, **20**, 1297.
119 M. Ganne, M. Dion, A. Boumaza and M. Tournoux, *Solid State Commun.*, 1986, **59**, 137.
120 L. Kihlborg, *Ark. Kemi*, 1963, **21**, 471.
121 M. H. Whangbo, M. Evain, E. Canadell and M. Ganne, *Inorg. Chem.*, 1989, **28**, 267.
122 A. Magnéli, *Acta Chem. Scand.*, 1948, **2**, 501.
123 (*a*) J. P. Giroult, M. Goreaud, Ph. Labbe and B. Raveau, *Acta Crystallogr., Sect. B*, 1981, **37**, 2139; (*b*) B. Domenges, F. Studer and B. Raveau, *Mater. Res. Bull.*, 1983, **18**, 669.

Paper 7/03996D; *Received* 9*th June*, 1997